

# MFIE-Based Propagation Prediction

Fernando J. S. Moreira

**Abstract**— This work presents a MFIE-based prediction for vertically polarized radio waves propagating over a smoothly irregular terrain. The present theory is compared against its EFIE counterpart. It is shown that the MFIE-based technique yields accurate predictions with less basis functions than the EFIE one, specially for those regions where the line-of-sight is obstructed.

**Keywords**— Electromagnetic propagation, UHF radio propagation, integral equation.

## I. INTRODUCTION

Accurate characterizations of radio-wave channels are constantly demanded by the growth of wireless services and the associate restrictions imposed upon the required spectrum. Among the possible techniques, special attention is being devoted to the integral equations due to their inherent full-wave analysis. Recently, Hviid *et. al* [1] proposed a technique based on the electric field integral equation (EFIE) for vertically polarized wave propagation over smoothly irregular terrains. By neglecting the back scattering mechanisms, a forward scheme could be implemented in order to obtain the induced currents recursively, without the need of a moment-method (MoM) full-matrix treatment. Accelerating techniques have also been proposed [2], enabling the propagation prediction over large distances.

In the present work, a magnetic field integral equation (MFIE) technique is presented and compared against the EFIE one for a representative case study. It is demonstrated that the MFIE yields the same level of accuracy as the EFIE, but with less basis functions for the description of the induced currents, specially for those regions where the line-of-sight (LOS) is obstructed. Consequently, the MFIE yields a large reduction in computer time, being suited for large-distance coverage predictions.

## II. MFIE FOR A VERTICAL POLARIZATION

An EFIE-based propagation prediction for vertically polarized radio waves was presented and discussed in [1]. Basically, a surface integral equation was employed to solve for the equivalent currents induced over the ground. For vertical polarization, near-grazing incidence, and neglecting any losses, the terrain was treated as a perfect magnetic conductor (PMC) and the boundary conditions were imposed by means of equivalent magnetic surface currents. Furthermore, the terrain was assumed smooth along the plane of incidence and perpendicular invari-

ant. This enabled the application of a stationary phase method (SPM) to solve for the integral along the perpendicular direction, thus reducing the problem into a 1-D one. The induced magnetic currents could then be obtained via the usual MoM matrix equation. However, by assuming a smooth profile and neglecting the back scattering, the upper-triangular portion of the impedance matrix becomes null and the magnetic-current coefficients were directly obtained via a forward scheme [1]. In the present work, the same treatment is applied but for the MFIE, which is discussed next.

For the problem at hand, only equivalent magnetic currents ( $\vec{M}$ ) are needed and the corresponding MFIE with suppressed time variation  $\exp(j\omega t)$  can be written as [3]

$$\vec{H}(\vec{r}) = T \left[ \vec{H}_{in}(\vec{r}) + \frac{1}{\eta} \vec{L}_1(\vec{M}) \right], \quad (1)$$

where  $\vec{H}_{in}$  is the incident magnetic field radiated by external sources,  $\eta$  is the free-space impedance,  $T = 1$  or  $2$  for an observer outside or at the (smooth) surface  $S$ , respectively,

$$\vec{L}_1(\vec{M}) = -jk \oint_{S'} \left[ \vec{M}(\vec{r}')G - \frac{1}{k^2} \nabla' \cdot \vec{M}(\vec{r}') \nabla' G \right] ds', \quad (2)$$

and

$$G = G(\vec{r}, \vec{r}') = \frac{\exp(-jk|\vec{r} - \vec{r}'|)}{4\pi|\vec{r} - \vec{r}'|} \quad (3)$$

is the free-space Green's function, where the prime coordinates locate the equivalent currents over  $S$ , as usual. One must bare in mind that, throughout this work, all the integrals over  $S$  are to be evaluated under the principal-value principle [3]. The induced currents  $\vec{M}$  are solved from (1) after imposing the boundary conditions upon the tangential field components over  $S$  [3]:

$$\hat{n} \times \vec{H}(\vec{r}) = 0 \quad \Rightarrow \quad \hat{n} \times \vec{H}_{in}(\vec{r}) = -\frac{1}{\eta} \hat{n} \times \vec{L}_1(\vec{M}), \quad (4)$$

where  $\hat{n}$  is the outwardly-directed normal vector.

## III. MOMENT-METHOD SOLUTION

The use of the MoM technique for solving integral equations is well known and will not be discussed in detail. Basically, the unknown current  $\vec{M}$  is first expanded into a series of  $N_b$  basis functions  $\vec{m}_j$ , multiplied by the corresponding coefficients  $M_j$ :

$$\vec{M}(\vec{r}') = \sum_{j=1}^{N_b} M_j \vec{m}_j(\vec{r}'). \quad (5)$$

Manuscript received on February 2, 2001.  
Fernando J. S. Moreira, Federal University of Minas Gerais, Dept. Electronic Engineering, Av. Pres. Antonio Carlos 6627, Pampulha, Caixa Postal 209, 30161-970 Belo Horizonte, MG, Brazil, Tel. (+5531) 3499-4861, FAX (+5531) 3499-4850, fernando@eee.ufmg.br.

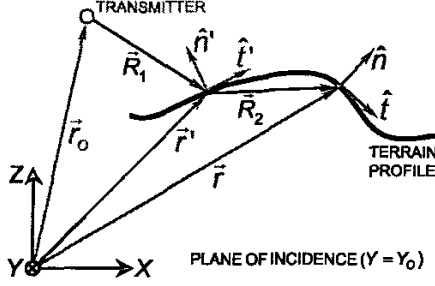


Fig. 1. Basic geometric parameters.

After substituting (5) into (4) and further taking the inner product of the resulting integral equation with a proper set of weighting functions  $\bar{w}_i$ , the (approximate) solution for  $\bar{M}$  is attained via the following matrix equation:

$$[V_i] = [Z_{ij}] [M_j], \quad (6)$$

where, after the multiplication of (4) by  $\eta$ ,

$$V_i = \eta \oint_S \bar{w}_i \cdot (\hat{n} \times \bar{H}_{in}) ds, \quad (7)$$

$$Z_{ij} = - \oint_S [\bar{I}_1(\bar{m}_j) \cdot (\bar{w}_i \times \hat{n}) + \mathcal{I}_2(\bar{m}_j) \nabla \cdot (\bar{w}_i \times \hat{n})] ds, \quad (8)$$

and

$$\bar{I}_1(\bar{m}_j) = -jk \oint_{S'} \bar{m}_j(\bar{r}') G(\bar{r}, \bar{r}') ds', \quad (9)$$

$$\mathcal{I}_2(\bar{m}_j) = \frac{j}{k} \oint_{S'} [\nabla' \cdot \bar{m}_j(\bar{r}')] G(\bar{r}, \bar{r}') ds'. \quad (10)$$

The integrals in (9) and (10) can be considerably simplified after the following assumptions are made. First of all, the most important contribution to the scattered field generally comes from the ground region around the plane of incidence, specially for narrow Fresnel zones [1]. So, as far as the lateral contributions can be neglected, the ground surface can be assumed invariant perpendicular to the plane of incidence. Thus, the integrals along this direction can be asymptotically evaluated by means of the stationary-phase method (SPM), as done in [1] for the EFIE.

To illustrate the procedure, it is assumed that the normal to the incidence plane is  $\hat{y}$ , as shown in Fig. 1. Besides,  $\bar{m}_j$  is conveniently rewritten as

$$\begin{aligned} \bar{m}_j(\bar{r}') &= [m_j^t(t', y') \hat{t}' + m_j^y(t', y') \hat{y}] e^{-jk|\bar{r}' - \bar{r}_o|} \\ &= (\bar{m}_j^t + \bar{m}_j^y) e^{-jk|\bar{r}' - \bar{r}_o|}, \end{aligned} \quad (11)$$

where  $\bar{r}_o$  is the position vector of the transmitting antenna (with Cartesian coordinates  $x_o$ ,  $y_o$ , and  $z_o$ ),  $t'$  and  $y'$  form a locally orthogonal coordinate system over  $S$  (at the source point) with unit vectors  $\hat{t}'$  and  $\hat{y}'$ , respectively,

and with  $\hat{n}' = \hat{t}' \times \hat{y}'$  being the surface unit normal, as depicted in Fig. 1. This also means that  $ds' = dt' dy'$  in (9) and (10), where the integrals with respect to  $y'$  will be evaluated by the SPM. In (11) the exponential term was put in evidence to stress the assumption of the equivalent-current phase being locally spherical, as it originates from a point source at  $\bar{r}_o$  [1].

Under these circumstances, (9) can be rewritten as

$$\bar{I}_1(\bar{m}_j) = -jk \int_{t'=-\infty}^{\infty} \int G(\bar{r}, \bar{r}') (\bar{m}_j^t + \bar{m}_j^y) e^{-jk|\bar{r}' - \bar{r}_o|} dy' dt', \quad (12)$$

which, after applying the SPM to evaluate the  $y'$ -integral, is reduced into [1]

$$\bar{I}_1(\bar{m}_j) \approx -jk \int_{t'} G(R_1, R_2) (\bar{m}_j^t + \bar{m}_j^y) \Big|_{y'=y_o} dt', \quad (13)$$

where (see Fig. 1)

$$G(R_1, R_2) = \frac{\exp[-jk(R_1 + R_2) - j\pi/4]}{4\pi\sqrt{(1 + R_2/R_1)R_2/\lambda}}, \quad (14)$$

$$R_1 = |\bar{r}' - \bar{r}_o|_{y'=y_o} = \sqrt{(x' - x_o)^2 + (z' - z_o)^2}, \quad (15)$$

$$R_2 = |\bar{r} - \bar{r}'|_{y'=y'=y_o} = \sqrt{(x - x')^2 + (z - z')^2}. \quad (16)$$

Also, (10) can be rewritten as

$$\begin{aligned} \mathcal{I}_2(\bar{m}_j) &= \frac{j}{k} \int_{t'=-\infty}^{\infty} \int G(\bar{r}, \bar{r}') \\ &\times \nabla' \cdot [(\bar{m}_j^t + \bar{m}_j^y) e^{-jk|\bar{r}' - \bar{r}_o|}] dy' dt', \end{aligned} \quad (17)$$

where

$$\begin{aligned} \nabla' \cdot [(\bar{m}_j^t + \bar{m}_j^y) e^{-jk|\bar{r}' - \bar{r}_o|}] &= \\ \left[ -jk (\bar{m}_j^t + \bar{m}_j^y) \cdot \frac{(\bar{r}' - \bar{r}_o)}{|\bar{r}' - \bar{r}_o|} + \frac{\partial m_j^t}{\partial t'} + \frac{\partial m_j^y}{\partial y'} \right] e^{-jk|\bar{r}' - \bar{r}_o|}. \end{aligned}$$

The evaluation of the  $y'$ -integral in (17) by the SPM gives

$$\begin{aligned} \mathcal{I}_2(\bar{m}_j) &\approx \frac{j}{k} \int_{t'} G(R_1, R_2) \left( -jk \bar{m}_j^t \cdot \hat{R}_1 \right. \\ &\left. + \frac{\partial m_j^t}{\partial t'} + \frac{\partial m_j^y}{\partial y'} \right) \Big|_{y'=y_o} dt', \end{aligned} \quad (18)$$

where (see Fig. 1)

$$\hat{R}_1 = \frac{(\bar{r}' - \bar{r}_o)}{|\bar{r}' - \bar{r}_o|} \Big|_{y'=y_o} = \frac{(x' - x_o) \hat{x} + (z' - z_o) \hat{z}}{R_1}, \quad (19)$$

and noticing that  $\bar{m}_j^y \cdot \hat{R}_1 = 0$  when  $y = y_o$ . Furthermore, under the present assumptions the induced magnetic current is oriented along the  $\hat{y}$ -direction at  $y' = y_o$  (i.e.,  $\bar{m}_j^t = 0$  at  $y' = y_o$ ) [1]. This symmetry also implies

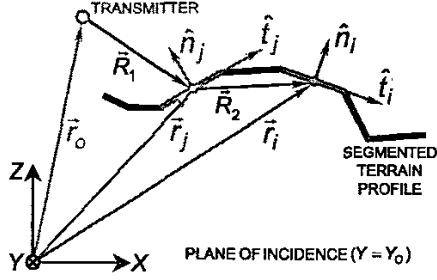


Fig. 2. Segmented terrain profile.

on a quasi null  $\nabla \cdot \vec{m}_j$  along the plane of incidence and, consequently,

$$\left( -jk \vec{m}_j \cdot \hat{R}_1 + \frac{\partial m_j^x}{\partial t'} + \frac{\partial m_j^y}{\partial y'} \right)_{y'=y_0} = 0,$$

meaning that, from (13) and (18),

$$\tilde{I}_1(\vec{m}_j) \approx -jk \int_{y'} \mathcal{G}(R_1, R_2) m_j^y(t') \hat{y} dt', \quad (20)$$

$$I_2(\vec{m}_j) \approx 0. \quad (21)$$

It is important to observe that, after the evaluation of the  $y'$ -integrals by the SPM, the solution of the integral equation just need to be imposed upon the terrain profile at  $y = y_0$ . Consequently, the surface integrals with respect to the observation point in (7) and (8) are reduced into line integrals with respect to  $t$  (the observation coordinate along the profile, as indicated in Fig. 1). Finally, in (20) one must be concerned with the singularities present whenever  $R_2 \rightarrow 0$  (see Fig. 1). The way to overcome such singularities depends on how the MoM technique is conducted. This is stressed in the next section for the particular case to be considered.

#### IV. PULSE BASIS FUNCTION AND POINT MATCHING

The solution of the present MFIE will be conducted as done in [1] for the EFIE. Defining  $\vec{w}_i$  parallel to  $\vec{m}_j$  (i.e.,  $\vec{w}_i = w_i \hat{y}$ ) and after straightforward manipulations upon (7), (8), (20), and (21), the MoM matrix elements can be rewritten as

$$V_i \approx \eta \int_t w_i(t) (\hat{y} \cdot \vec{H}_{in}) dt, \quad (22)$$

$$Z_{ij} \approx jk \int_t \int_{t'} w_i(t) m_j^y(t') \mathcal{G}(R_1, R_2) dt' dt. \quad (23)$$

The use of the standard MoM technique for practical links demands an overwhelming computational effort, due the tremendous number of unknowns to be determined. To simplify the formulation, the integration path along the terrain profile is subdivided into several straight segments, as illustrated in Fig. 2. Furthermore, point-matching is applied, meaning that  $w_i$  is a Dirac delta function defined

at the center of each observation segment ( $i$ -segment). Finally, the local basis functions are specified as  $m_j^y = 1$  over the source segment ( $j$ -segment) and zero elsewhere. After such definitions, (22) simplifies into

$$V_i \approx \eta \hat{y} \cdot \vec{H}_{in}(\vec{r}_i), \quad (24)$$

where  $\vec{r}_i$  locates the center of the  $i$ -segment (see Fig. 2). For the integrals with respect to  $t'$  in (23), the length ( $\Delta_j$ ) of the  $j$ -segment is assumed sufficiently small and the integrand a constant one, given by its value at  $\vec{r}_j$  (see Fig. 2). So, from (23) and for  $i \neq j$ ,

$$Z_{ij} \approx jk \mathcal{G}(R_1, R_2) \Delta_j, \quad (25)$$

where now, with the help of (15), (16), and Fig. 2,

$$\vec{R}_1 = R_1 \hat{R}_1 = \vec{r}_j - \vec{r}_o, \quad (26)$$

$$\vec{R}_2 = R_2 \hat{R}_2 = \vec{r}_i - \vec{r}_j. \quad (27)$$

However, caution should be taken whenever  $i = j$ . In such case, as  $R_2 \rightarrow 0$  and from (14), (20) reduces into

$$\begin{aligned} \tilde{I}_1(\vec{m}_j) &\approx -\frac{e^{j\pi/4} e^{-jkR_1}}{2\sqrt{\lambda}} \hat{y} \int_{t'} \frac{dt'}{\sqrt{R_2}} \\ &= -(1+j) \sqrt{\frac{\Delta_j}{\lambda}} e^{-jkR_1} \hat{y}, \end{aligned} \quad (28)$$

and from (23), when  $i = j$ ,

$$Z_{ii} \approx (1+j) \sqrt{\frac{\Delta_j}{\lambda}} e^{-jkR_1}. \quad (29)$$

#### V. FORWARD SCHEME

The standard MoM solution demands an overwhelming effort, specially for electrically-large terrain profiles. As far as such profiles can be treated as (electrically) smooth and no large obstacles (like steep mountains) are present, the back scattering may be neglected [1]. Mathematically, this means that the  $Z_{ij}$ -elements of the upper-triangular portion of the impedance matrix can be assumed zero and, consequently, the solution for the unknown coefficients  $M_j$  is straightforward:

$$M_i = \frac{1}{Z_{ii}} \left( V_i - \sum_{j=1}^{i-1} Z_{ij} M_j \right), \quad (30)$$

with  $i$  being sequentially varied from 1 to  $N_b$ . Once the induced currents are obtained the scattered field can be determined as in [1].

#### VI. THE HJØRRINGVEJ PROFILE

Several case studies were investigated and demonstrated that the MFIE-based technique is capable of yielding the same accuracy as the EFIE one but with a reduced number ( $N_b$ ) of segments. To illustrate this fact, Fig. 3 shows

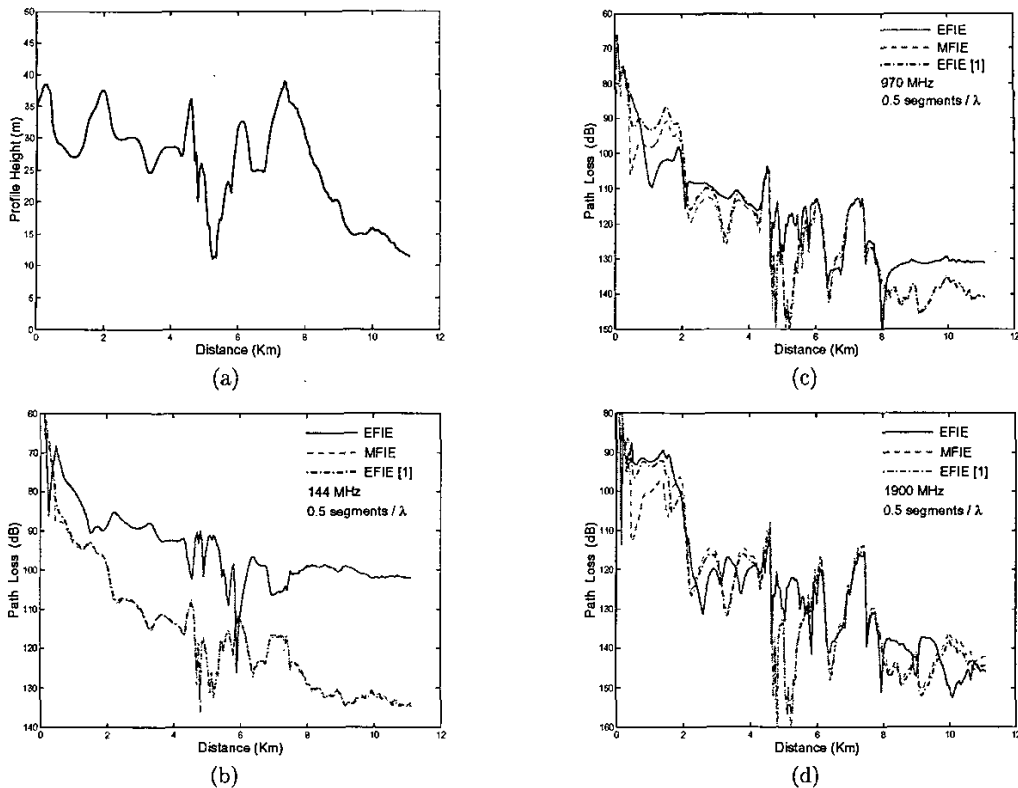


Fig. 3. Path loss predictions for "Hjørringvej" [1]: a) terrain profile and results for b) 144 MHz, c) 970 MHz, and d) 1900 MHz.

the path-loss predictions for the Hjørringvej profile investigated in [1]. The transmitter was placed 10 m above the profile, at its beginning. The receiver was 2.4 m above the profile depicted in Fig. 3(a). So, one observes that the LOS becomes obstructed after a distance of 2 km. The profile was subdivided into 0.5 segments per wavelength for each different frequency. The numerical predictions given by both the EFIE and the MFIE are depicted in Figs. 3(b), (c), and (d) at 144, 970, and 1900 MHz, respectively, where they are being compared against those of [1]. From these figures one observes that, even when a small number of segments is used to describe the induced currents, the MFIE still sustains the desired accuracy, specially at the region where the LOS is obstructed. Furthermore, the results at 1900 MHz indicate that a larger number of segments shall be used as the frequency increases. However, the MFIE still requires a smaller  $N_b$  number than the EFIE.

## VII. CONCLUSIONS

This work presented a MFIE-based technique for the UHF coverage prediction of a vertically polarized wave propagating over smoothly irregular terrains. Horizontally polarized waves can be treated likewise by

invoking the duality principle. It was verified that the MFIE-based prediction provides the same level of accuracy as the EFIE but with less basis functions used to describe the induced currents, specially when the line-of-sight is obstructed. The results indicate the high potentiality of the MFIE-based technique for predictions over large terrain profiles due to the consequent reduction of the computation burden. Available accelerating techniques can also be adopted to speed up the process.

## ACKNOWLEDGMENT

The author would like to thank Prof. J. B. Andersen for providing the data of the Hjørringvej profile and the numerical predictions presented in [1].

## REFERENCES

- [1] J. T. Hviid, J. B. Andersen, J. Toftgård, and J. Bøjer, "Terrain-Based Propagation Model for Rural Area—An Integral Equation Approach," *IEEE Trans. Antennas Propagat.*, vol. 43, pp. 41–46, Jan. 1995.
- [2] C. Brennan and P. J. Cullen, "Multilevel Tabulated Interaction Method Applied to UHF Propagation over Irregular Terrain," *IEEE Trans. Antennas Propagat.*, vol. 47, pp. 1574–1578, Oct. 1999.
- [3] A. J. Poggio and E. K. Miller, *Computer Techniques for Electromagnetics*. Oxford, U.K.: Pergamon, 1973, ch. 4.